Cover Page

Universiteit Leiden

The handle http://hdl.handle.net/1887/21704 holds various files of this Leiden University dissertation

Author: Gupta, Vikas
Title: Multimodality cardiac image analysis for the assessment of coronary artery disease
Issue Date: 2013-09-11

5

Comprehensive visualization of multimodal cardiac imaging data for assessment of coronary artery disease: first clinical results of the SMARTVis tool

Abstract

In clinical practice, both coronary anatomy and myocardial perfusion information are needed to assess coronary artery disease (CAD). The extent and severity of coronary stenoses can be determined using computed tomography coronary angiography (CTCA); the presence and amount of ischemia can be identified using myocardial perfusion imaging, such as perfusion magnetic resonance imaging (PMR). To determine which specific stenosis is associated with which ischemic region, experts use assumptions on coronary perfusion territories. Due to the high variability between patient's coronary artery anatomies, as well as the uncertain relation between perfusion territories and supplying coronary arteries, patient-specific systems are needed. We present a patient-specific visualization system, called Synchronized Multimodal heART Visualization (SMARTVis), for relating coronary stenoses and perfusion deficits derived from CTCA and PMR, respectively. The system consists of the following comprehensive components: (1) two or three-dimensional fusion of anatomical and functional information, (2) automatic detection and ranking of coronary stenoses, (3) estimation of patient-specific coronary perfusion territories. The potential benefits of the SMARTVis tool in assessing CAD were investigated through a case-study evaluation (conventional vs. SMARTVis tool): two experts analyzed four cases of patients with suspected multivessel coronary artery disease. When using the SMARTVis tool, a more reliable estimation of the relation between perfusion deficits and stenoses led to a more accurate diagnosis, as well as a better interobserver diagnosis agreement. The SMARTVis comprehensive visualization system can be effectively used to assess disease status in multivessel CAD patients, offering valuable new options for the diagnosis and management of these patients.

CORONARY artery disease (CAD) Coronary artery disease (CAD) is a major cause of death worldwide [11]. Oxygen and nutrients, which are required for normal heart function, are supplied to the myocardium (i.e. the heart muscle) by the blood traveling through the coronary arteries. If a coronary artery becomes narrowed or occluded with build-up of plaque (e.g. cell, fat and cholesterol), the amount of blood flowing to the myocardium is reduced and, thus, less oxygen and nutrients are delivered to these myocardial regions. The restriction in blood and oxygen is called *ischemia* and the narrowing of vessel is called *stenosis*. Coronary artery stenoses can either cause temporary changes to these ischemic myocardial regions or, if the myocardium is not supplied with sufficient blood during a too long period, can cause death of the myocardial tissue, which can lead to myocardial infarction.

Many tests are available for detecting and diagnosing CAD, such as electrocardiograms, exercise stress tests, echocardiograms, nuclear scan tests, stress thallium tests and angiography. Each of these tests has unique advantages, the choice of which (and how many) tests to perform is determined by the patient's history and current symptoms. In current clinical practice, angiography is the gold standard imaging technique for diagnosing CAD; the location, the number and the severity of the vessel stenoses can be determined. Nevertheless, computed tomography coronary angiography (CTCA) imaging technique is gaining popularity [256]; it (non-invasively) provides high-resolution images of the cardiac and coronary artery anatomy, which allow assessment of the presence, extent and type (calcified or non-calcified) of coronary plaques (i.e. stenoses). Depending on the location and information regarding the severity of the stenoses, an ischemic test may be required to evaluate if, and to what extent, the obstruction is causing a perfusion defect. Cardiac perfusion magnetic resonance imaging (PMR) is one of the possible ischemic tests; PMR can be used to measure the global and regional myocardial perfusion of the heart [123, 125], and thus provides information on myocardial perfusion abnormalities (i.e. presence of ischemia).

CTCA images are analyzed using different visualization techniques, such as multi-planar reformatted (MPR) and curved-planar reformatted (CPR) images; MPR and CPR images are oblique views obtained from axial sections of the CTCA images (see Figure 5.1). Conventionally, the interpretation of left ventricular function is performed by visually checking the cardiac PMR images (under rest and stress) and by looking at time-intensity curves (TIC) and perfusion-linked parameters on a bull's eye plot (BEP). Figure 5.2 presents an example of these representations. A BEP is a two dimensional (2D) representation of the three dimensional (3D) myocardium; the left ventricle, which has an ellipsoid shape, is unfolded to a disc. The short-axis left ventricle sections are displayed with rings on the 2D BEP: the most apical slice is plotted at the center, while the most basal slice forms the outermost ring of the BEP.

After independently viewing the CTCA and PMR images, the expert needs to *mentally* integrate anatomical and functional information: each myocardial defect has to be assigned to a culprit coronary artery, in order to determine which coronary artery stenoses are in fact hemodynamically significant (i.e. induce a perfusion defect). The potential improvement of decision-making in the management of patients is one of the most important reasons for use of integrated imaging; integration of data derived from these complementary (i.e. CTCA and PMR) techniques may offer valuable advantages in diagnosis, staging and treatment of CAD. Therefore, there is a need for visualization methods that integrate multimodal cardiac data.

Figure 5.1: Multiplanar reformatted view of a vessel in a computed tomography coronary angiography image. The pink cross on the long-axis view (right) shows the position of a calcified plaque. It is synchronized with the short-axis view (left), on which the vessel segmentation (red contour) is overlaid.

The American Heart Association (AHA) has published some recommendations concerning coronary artery perfusion territories, with respect to their standardized 17-segment BEP model [47]. However, because variability in coronary anatomy between patients can be high, the use of a standard model may not be optimal. For instance, Pereztol et al. [176] demonstrated that only nine of the 17 AHA-segments are fed by a single coronary artery, while the other eight segments may be fed by more than one coronary artery (Figure 5.3). If the patient only has a single obstructive lesion (i.e. single vessel disease, low-risk patient[1]), it is clear which coronary is causing the perfusion defect, and, thus, integrating information in a patient-specific way would lead to the same diagnosis. Also, symptomatic CAD patients at very-high-risk (i.e. with significant stenoses in the 3 main coronary arteries) would not benefit from such a combined approach, as they are usually immediately referred for revascularization. Consequently, integrating information in a patient-specific way is mainly beneficial in the diagnosis of *intermediate-risk patients*, who have suspected stenoses in 2 of the 3 main coronary arteries, as there may be ambiguous assignment of perfusion defects and culprit coronary arteries.

In this work, we present several visualization methods, implemented in the Synchronized Multimodal heART Visualization (SMARTVis) tool, that allow a comprehensive analysis of cardiac multimodal imaging data, for assessment of CAD. Our contribution is threefold:

- We present an innovative integration of image processing methods to (semi)-automatically analyze cardiac multimodal imaging data (e.g. heart segmentation, coronary centerline tracking and lumen segmentation from CTCA; registration and segmentation of PMR images).

- Using the results from the image processing stage, we present comprehensive visualizations for relating coronary stenoses and perfusion defect regions: 1) projection of the coronary artery tree onto a 2D BEP, 2) integration of the perfusion information into a 3D model of the heart, 3) automatic detection and ranking of coronary stenoses, 4) estimation (distance-based) of the patient-specific coronary perfusion territories, and 5) synchronization of the 2D and 3D viewers with CTCA and PMR images. To our knowledge, an integration of all of these elements into a single coordinated visual analysis tool is novel, maximizing the diagnostic complementarities of the imaging modalities.

---

[1]the *risk* refers to the pre-test probability of having CAD.
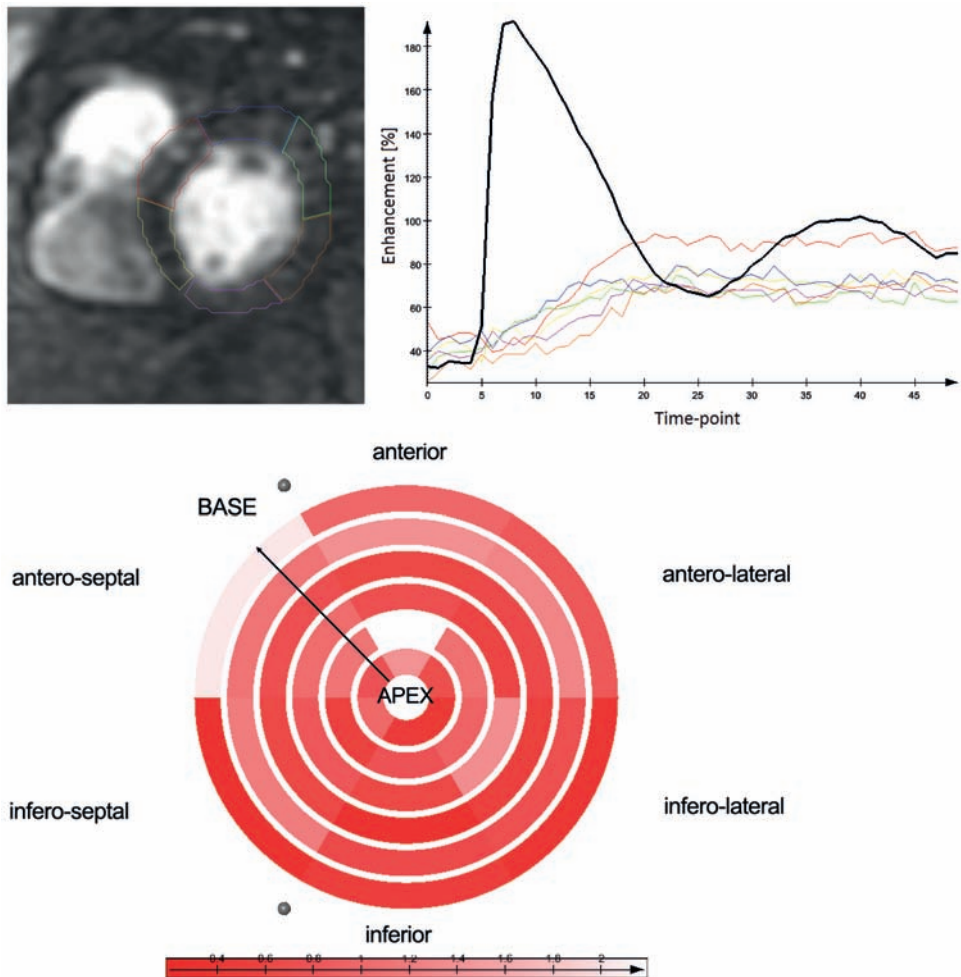
Figure 5.2: Example of a mid-ventricular stress perfusion magnetic resonance slice (top left), the corresponding signal-intensity versus time curves for 6 left ventricular segments (top right), derived from a motion-compensated PMR image sequence. The myocardial perfusion reserve index is visualized on the bull's eye plot (bottom).
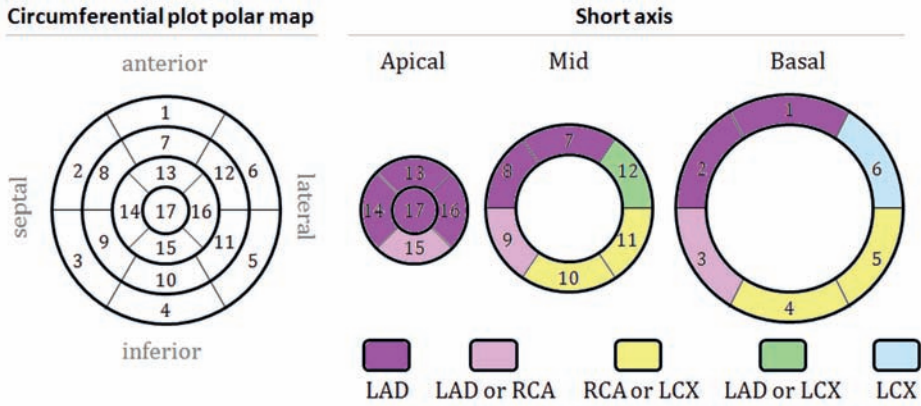
Figure 5.3: Correspondence between the 17 left ventricular myocardial segments and each coronary artery, according to results from [176].
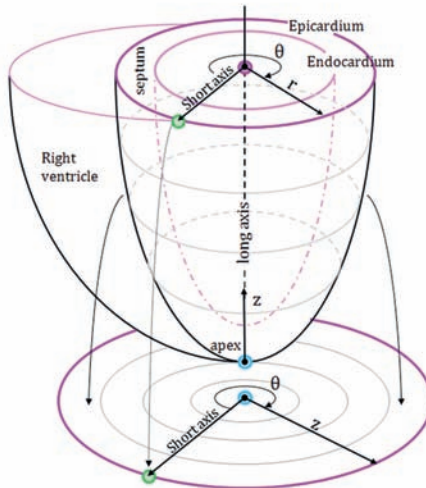
Figure 5.4: Common frame of reference - A bull's eye plot is a 2D representation of the myocardium; it is constructed by unfolding and reformatting the 3D elipsoid myocardium to a 2D circle. Adapted from Termeer*et al.* [233].

- Finally, we investigated the benefits of the SMARTVis tool in assessing CAD by performing both a comparative study and a case-study evaluation. Here, two experts analyzed four patients with suspected multivessel disease, using conventional tools and the SMARTVis tool.

Related work is discussed in the following section. In Section 5.2 we describe how information is extracted from multimodal imaging data and comprehensively visualized. Section 5.3 is dedicated to the evaluation of the SMARTVis tool. In Section 5.4, we discuss feedback from the expert clinicians and the limitations of our approach. Finally, Section 5.5 presents the conclusions and possibilities for future studies.

5.1 Related work

Currently, various methods exist to combine multimodal data and they can be divided in two groups: methods that are based on image fusion and ones that use models to integrate multimodal information.

Image fusion, which results in hybrid images, can be used to combine anatomic and functional data: Faber et al. [73] proposed a method to integrate the information from SPECT myocardial perfusion imaging (SPECT-MPI) with biplane X-ray angiograms, and Gaemperli et al. [81] suggested fusing SPECT-MPI with CTCA. Van Werkhoven et al. [247] demonstrated that CTCA has an incremental prognostic value over SPECT-MPI in patients with suspected CAD. More recently, the feasibility and potential value of the combined analysis of integrated anatomical and functional data have been discussed by Scholte et al. [206]; they concluded that SPECT-MPI/CTCA image fusion provides additional clinical value compared to the analysis of either technique alone or side-by-side. Nowadays, the introduction of SPECT-CT and PET-CT systems enables data to be acquired from both modalities in a single session, making hybrid image acquisition even easier.

Model-based visualization techniques can also be used to combine multimodal imaging data. Termeer et al. [233] proposed a comprehensive visualization framework, called CoViCAD, to combine multiple MR images. Here, coronary centerlines were extracted from a whole-heart MR scan and scar tissue was visualized in late-enhancement MR images. At that time, whole-heart MR technology did not provide enough spatial resolution to extract absolute diameter information for the coronary arteries. The coronary artery tree was therefore represented by constant radius tubes around the centerlines; thus, no indication about possible stenosis was provided. In the present work, two novel visualizations are provided: 1) the introduction of a 3D volumetric BEP, which preserves the volumetric nature of the left ventricular wall and thus allows better appreciation of transmurality information, and 2) the overlay of coronary arteries on the epicardial surface of the 3D volumetric BEP, providing additional contextual information.

Termeer et al. [234] also proposed visualization techniques to study the effect of coronary artery stenosis on myocardial perfusion, using a simulation approach. Here, a coronary tree, with absolute radius, was extracted from a single CTCA image. After simulating the blood flow in the coronary arteries with a numerical model, the simulated left ventricle perfusion was visualized on a 2D BEP; under-perfused regions and coronary artery blood supply territories were enhanced. However, such a model can only be used to observe the effect of stenoses. In fact, the presented computational simulation of perfusion has not been validated (i.e. compared with true perfusion values extracted from

perfusion imaging such as PMR or SPECT) and, therefore, there is no guarantee that the presented perfusion values correspond closely to the reality.

This limitation has been addressed by Kühnel et al. [132, 133]. They combined anatomical information derived from CTCA with scar tissue information extracted from LE-MRI images and perfusion information from PMR images. Various 2D and 3D visualizations were proposed to emphasize suspicious myocardial regions: 1) overlaying of the coronary tree mask and scar tissue directly on the 2D LE-MRI images, 2) integration of functional information with a 3D model of the coronary artery tree, 3) incorporation of a selected 2D LE-MRI slice into the 3D model, 4) interaction with the 2D BEP, and 5) detection of findings. However, neither a mapping of the coronary arteries on top of the 2D BEP nor a 3D model of the heart was provided.

The present work is an extension of our earlier work [121]; here, we focus on model-based visualization techniques to combine CTCA and PMR imaging data. Within this context, we have implemented a number of existing comprehensive visualization techniques within the SMARTVis tool [132, 133, 234]: projection of the coronary artery tree onto the 2D BEP, integration of the functional information into a 3D model, a coronary perfusion territory map, multiple linked views (2D, 3D and MPR viewers) and animation (automatic camera position). However, we also overcome the limitation encountered by Termeer et al. [233] [234], as we are able to: 1) reconstruct and project the coronary artery tree with absolute diameter, and 2) analyze the impact of coronary artery stenoses on myocardial perfusion derived directly from PMR instead of a simulated model. The main novelty of the presented work compared to [121] is the case-study clinical evaluation, in which we investigated whether integration of coronary anatomy and myocardial perfusion data can improve risk assessment, diagnosis and management of patients with CAD. In addition, the computation of patient-specific perfusion territories (Section 5.2.5.2), as well as the automatic detection and stenosis quantification (Section 5.2.5.1), constitute the technical innovation compared to our previous work [121].

5.2 Method

An overview of the multimodal image analysis and fusion is presented in Figure 5.5. First, CTCA and PMR images were analyzed separately. Then, anatomical information extracted from CTCA was combined with functional information derived from PMR images. Finally, comprehensive visualization techniques were used to facilitate the joint analysis of coronary stenoses and myocardial perfusion defect.

5.2.1 CTCA image analysis

In daily clinical practice, CTCA images are analyzed using different visualization techniques, such as MPR and CPR (Figure 5.1), in order to detect vessel stenoses. MPR and CPR images are oblique views obtained from axial sections of the CTCA images and, thus, their generation requires vessel centerlines.

In our work, the semi-automatic method proposed by Metz et al. [151] was used to extract vessel centerlines: a minimum cost path approach was applied, in which the user interaction was minimized to two mouse clicks in the coronary arteries. First, a vesselness/intensity cost function was computed. Then, a point in the aorta close to the coronary ostia was user-defined to derive a cumulative cost-image; a point was also defined by the user distally, at the end of the coronary artery. The centerline was determined by following the path of steepest descent in the cumulative cost image to the
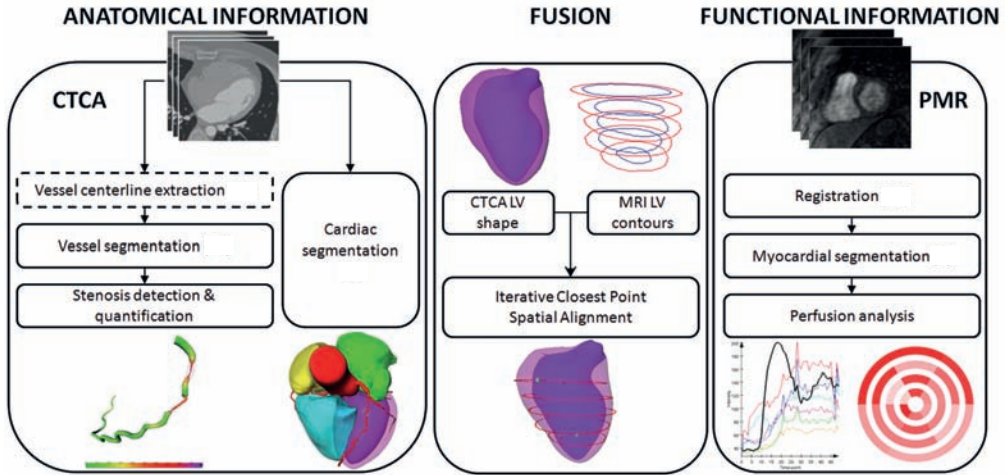
Figure 5.5: Overview of the multimodal image analysis and fusion. The dashed box corresponds to semi-automatic process, while the solid boxes correspond to fully automatic processes. Anatomical information is extracted from computed tomography coronary angiography (CTCA); functional information is extracted from perfusion magnetic resonance (PMR) imaging.

end point of the artery. The technique has been evaluated on images with a wide range of image qualities: good, adequate (i.e. presence of artifacts but evaluation possible with moderate confidence, poor (i.e. presence of image degrading artifacts and evaluation possible with low confidence). Also, the amount of pathology (i.e. calcification) present was considered in the evaluation. Results show that the method is able to cross regions suffering from bad image quality and pathological regions. The computation time for the centerline extraction was around 3 min for each of the three main arteries (LAD, RCA, LCX) and around 1.5 min for each side branch.

The resulting centerlines were used as an initialization for the segmentation of the coronary artery tree. Here, a recently introduced supervised shape-based segmentation method proposed by Schaap et al. [201] was used; the geometry and the appearance of the vessels were learned from annotated data. First, the vessels were segmented with multivariate linear regression, using image intensities sampled in a region of interest around the initial centerlines. Then, the position of the vessel boundaries was refined with a robust non-linear regression technique, using image intensities sampled on the boundary of the rough segmentations. The computation time for the lumen segmentation required 10-15 min per dataset, depending on the number of vessels to segment. This step was followed by a visual inspection and manual refinement of the lumen segmentation where needed.

Additionally, a 3D model of the heart, which includes ventricles, atria and aorta, was derived automatically from CTCA data, using the multi-atlas based segmentation approach presented in Kirişli et al. [120]. The cardiac segmentation method has been evaluated on a multicenter/multivendor database of 855 patients (1420 diastolic/systolic images), including patients of different age, gender, and ethnicity; the population is

also representative for the typical variability in cardiac anatomy, image quality, patient position, and orientation. Experts evaluated that 49% of the images were very accurately segmented (less than 1 mm error) and that 29% were accurately segmented (error between 1 and 3 mm), which demonstrates the robustness of the presented method. The authors reported 1% failure, due to significant differences in cardiac morphology, such as left pneumonectomy, aortic aneurysm, and congenital heart disease. The cardiac segmentation was on average performed within 20 min.

Finally, as the centerline tracking and lumen segmentation can be run concurrently with the cardiac segmentation, the entire CTA processing can be performed within 20-30 min, depending on the number of coronary arteries processed.

5.2.2 Cardiac perfusion MR image analysis

Cardiac PMR provides information about myocardial perfusion. In clinical practice, physiologically relevant features, together with their time-intensity behavior, are extracted from the PMR images, which require tracking of regional myocardial intensity in all the frames of a perfusion sequence as a function of time.

In this work, the fully automatic framework was used to analyze the PMR images. First, because the intensity signal must be derived from the same myocardial region in successive frames, the PMR images were compensated for respiratory motion using a registration method based on independent component analysis [154]. Subsequently, the registered data were used to automatically segment the myocardium with active appearance models [93]. Registration failures may occur when images of poor quality or presenting large breathing motion are processed. When registration failures occurred, the commercial QMass MR software (Medis Medical Imaging Systems B.V., Leiden, The Netherlands) was used to segment the myocardium. This happened during the analysis of the stress PMR sequence of one patient presenting large breathing motion.

Finally, given the myocardium segmentation, time-intensity curves (TIC) and perfusion parameters were computed (with QMass MR): baseline signal intensity (signal intensity value before the first-pass of the contrast agent), peak enhancement (PE) or amplitude (maximal signal intensity value normalized by the baseline value), mean intensity (mean intensity during the first-pass of contrast-agent), time to (50%) of PE (time between the start of the first-pass and the time at which (50% of) PE is achieved), upslope (maximum steepness during the first-pass of contrast-agent). The upslope of the myocardial TIC was normalized with the upslope of the left ventricular blood pool signal, and is referred to as the *relative upslope*. The myocardial perfusion reserve index (MPRI) was calculated by dividing the segment's relative upslope of the stress TIC by the corresponding segment's relative upslope of the rest TIC. For each slice consisting of 50 frames, the process of registering all the frames, obtaining the myocardial contours, and deriving the perfusion parameters takes (on average) 1.5 min. For datasets with 4-6 slices, the entire PMR processing thus requires 6-9 min.

5.2.3 Data fusion and integration

Because CTCA and PMR images were acquired at different imaging devices and at different times, some spatial registration is needed in order to combine the complementary information of coronary anatomy and myocardial perfusion imaging.

In this work, we used an iterative closest point (ICP) approach, in which an affine transformation is determined. The ICP algorithm requires a set of moving points $m \in M$,

points from PMR epicardial contours, and a set of target points $t \in T$, points from the 3D CTCA epicardium model. The transformation is initialized by aligning the centers of gravity of both point sets; this results in two new sets of points M_0 and T_0. Given a user-defined maximum number of iterations ($N = 100$) and/or a maximum distance ($\epsilon = 1.10^{-5}$) as stopping criterion, the iterative procedure will search for the affine transformation that minimizes the distance between each $m \in M_i$ and $T \in T_0$, M_i being the set of moving points after the ith iteration. The ICP alignment of the CTCA and PMR data is performed within a minute.

5.2.4 Coordinated and multiple views

A common frame of reference, adapted from Termeer et al. [233] (Figure 5.3) and based on the segmentation of the left ventricle, was used to combine the information extracted from the CTCA and PMR data. Each point of the CTCA image, particularly those on the myocardium and vessels, can be parameterized using cylindrical coordinates (ρ,θ,z), where **z** represents the left ventricle long-axis, θ represents the angle with the short-axis and ρ represents the distance to the long-axis. This 3D model is then unfolded along the left ventricle long-axis, to fit the 2D model of a BEP. Here, the radius of the disc corresponds to the z value and the angle to the θ values. The third dimension, ρ, is encoded in the rendering: the more transparent the artery is, the further it is from the left ventricle epicardial surface.

Upon establishing 2D-3D correspondence, an interesting position such as a stenosis located on the 3D (resp. 2D) model can be simultaneously located on the 2D (resp. 3D) model. Additionally, the MPR view of the vessel is interactive: by moving the cursor along the MPR images, the actual position along the vessel is simultaneously indicated on both the 2D and 3D models. Moreover, to facilitate the 3D navigation by the expert, the optimal camera position in the 3D model is automatically updated, given the MPR cursor position. Finally, the integration of a selected 2D CTCA slice in the 3D model is possible.

5.2.5 Visualization for comprehensive analysis

An overview of the proposed comprehensive visualizations is presented in Figure 5.6.

5.2.5.1 Automatic detection of stenosis

Given the vessel segmentation obtained from the CTCA data, the cross-sectional area A_z of the vessel was computed at every position z along the vessel centerline, $z \in [1, L]$ and L being the number of positions along the centerline. Given the assumption that a vessel is a tubular structure, the radius was then derived as follows: for all z between 1 and L, $r_z = \sqrt{A_z/\pi}$. To compute the degree of stenosis, the radius of a healthy vessel is needed, as a reference. Here, we estimated the radius of the healthy vessel by applying a robust weighted Gaussian kernel regression [60] to the 1D function describing the vessel radius r_z along the centerline, given a set of weights w_z.

The estimated healthy radius $\tilde{r}_z$ is represented by the dotted black line in Figure 5.7. The degree of stenosis $d_z = (\tilde{r}_z - r_z)/\tilde{r}_z$ was smoothed with a Gaussian kernel to remove noise and to avoid multiple detection of the same stenosis; it is represented by the red line. Given a threshold for significance of a stenosis $d_{max} = 0.3$, local maxima z_{max}^i with $d_{z_{max}^i} > 0.3$ were considered as stenosis positions. Here, the vessel presents two significant stenoses. For each patient of our study, all the coronary arteries were analyzed and the estimated significant stenosis were listed and ranked. Visually, the degree of stenosis can
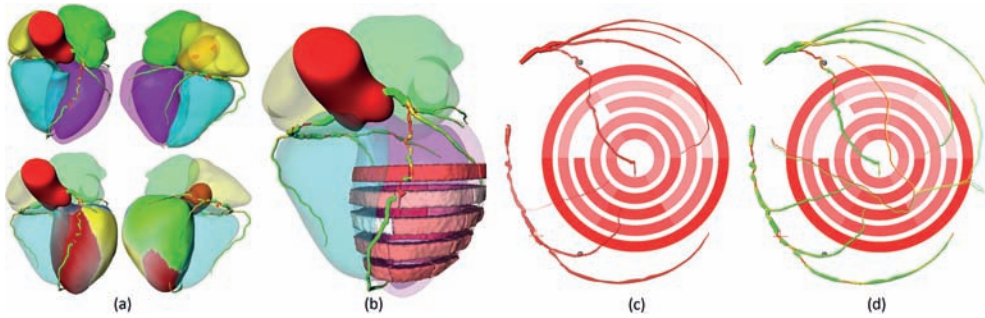
Figure 5.6: Comprehensive visualizations proposed in the SMARTVis tool - (a) 3D model of the heart and coronary artery tree extracted from CTCA, arteries are color coded with the degree of stenosis. Also, patient-specific perfusion territories are shown on the left ventricle (LAD in red, LCX in blue, MO in yellow and RCA in green). (b) 3D model of the heart with perfusion information integrated. (c) 2D perfusion bull's eye plot (BEP) with coronary tree projected on top; the more transparent the artery, the further it is from the epicardium. (d) 2D perfusion BEP with coronary tree and coronary perfusion territories projected on top; arteries are color coded with the degree of stenosis. The spheres next to the 2D BEP indicate the position of connection with the right-ventricle
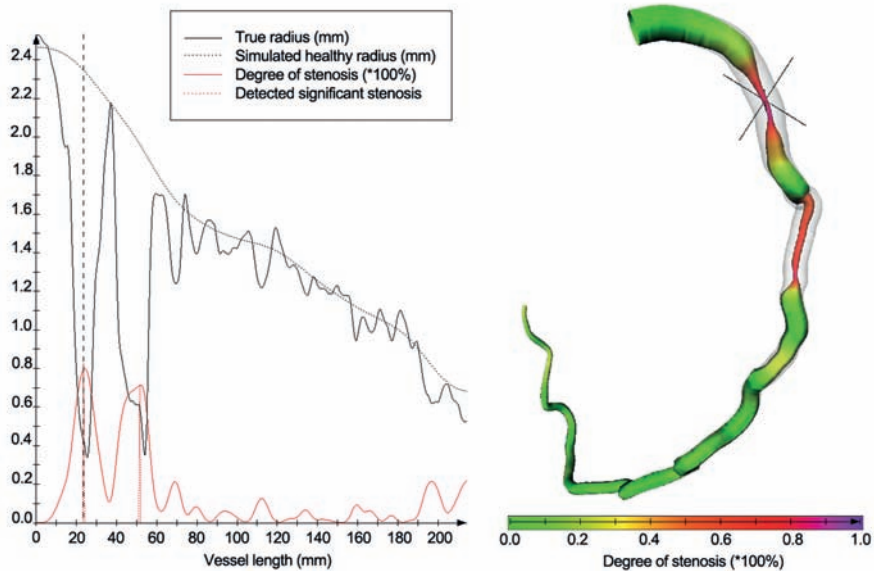
Figure 5.7: Automatic stenosis detection - The radius of a healthy vessel segment (black dotted line) is estimated by applying a robust weighted Gaussian kernel regression to the actual vessel radius (solid black line). The degree of stenosis can then be derived (solid red line) and significant stenoses (30%) are automatically detected (dotted red picks). The degree of estimated stenosis can then be visualized in 3D.

be color coded, which allows the expert to obtain a rapid first impression of the patient's degree of disease.

5.2.5.2 Patient-specific coronary territory map

In our work, we applied the method presented in Beliveau et al. [26] to compute patient-specific coronary perfusion territories from CTCA. From our left ventricular epicardial segmentation derived from CTCA, a 3D triangulated left ventricle shape S was created, with a maximum edge length of $2mm$. Then, all the coronary artery centerlines were projected onto S using the closest point method, except centerline points from the right coronary artery (RCA) that are more than $2cm$ from the myocardium. Subsequently, the shortest path (the geodesic distance over the surface) to each of the projected coronary arteries was computed for each node of S, using Dijkstra's algorithm; each node was then associated with the closest projected coronary. Examples of 3D coronary perfusion territories are shown on Figure 5.6 (two models at the bottom left): the red area is perfused by the left anterior descending (LAD) coronary artery , the yellow area by the marginal branch (MO), the blue area by the left circumflex artery (LCX) and the green area by the RCA. The purple region corresponds to the uncertain area (i.e. the left main branch, common to LAD, MO and LCX). The boundary between territories is represented by white dots. The nodes of the boundary can be expressed in cylindrical coordinates (ρ, θ, z) and can be projected onto the 2D BEP; Figure 5.6d shows an example.

5.2.5.3 Comprehensive 2D model

As in the comprehensive visualization proposed in Termeer et al. [233], the coronary arteries are projected onto the conventional 2D perfusion BEP, giving additional context information. Each point of the vessel centerlines c_i, $i \in [1, L]$, is parameterized to (ρ_i, θ_i, z_i) using the coordinate system presented in Section 5.2.4 and the radius r_i is stored. Using the same unfolding, the points c_i are projected to c_i' onto the 2D BEP. The coronary arteries are then reconstructed by creating tubes with center c_i' and radius r_i. In Figure 5.6c, the distance to the myocardium is encoded into the rendering: the more transparent the artery is, the further it is from the left ventricle epicardium surface. Here, the right artery is more transparent compared to other branches; in fact, the right artery runs through the right atrioventricular groove before approaching the left ventricle and, usually, only the distal branches of the RCA are actually close to the left ventricle. However, as a stenosis may occur in any position in the RCA, it is important to show the complete artery on the 2D model, and not only the distal part of the RCA. In Figure 5.6d, the coronary arteries are color-coded with their estimated degree of stenosis, and the patient-specific coronary perfusion territories can be overlaid too.

5.2.5.4 Comprehensive 3D model

Figure 5.6a presents examples of a 3D model of the heart with the coronary artery tree and the (optional) coronary perfusion territories mapped onto the LV. The coronary artery tree is color coded with the estimated degree of stenosis. Figure 5.6b shows a 3D model of the heart with integrated perfusion information derived from PMR. Such an integrated visualization provides a direct 3D correspondence between the vessel and the myocardial region supplied by the vessel.

5.2.6 Implementation

The development of the SMARTVis visualization and analysis tool was done using MeVisLab (http://www.mevislab.de), a rapid prototyping platform designed for (medical) image processing and visualization. The automatic detection of stenoses and computation of patient-specific coronary perfusion territory maps, as well as the cylindrical parameterization, were developed in C++. Additional dynamic functionalities were added to our graphical user interface using Python or JavaScript.

5.3 Evaluation

5.3.1 Data

Our patient population is a subset of the 50 patients included in the study of Kirschbaum et al. [125], in which they compared adenosine PMR imaging with invasive fractional flow reserve (FFR). Fifty symptomatic patients with suspected CAD and normal left ventricular ejection fraction who were referred for invasive coronary angiography (ICA) were asked to participate in the study. All of them underwent adenosine cardiac PMR imaging and ICA within 4 weeks. ICA was part of the routine clinical management, and functional assessment (FFR) was performed for vessel(s) which had a stenosis estimated as being larger than 30% as visualized on ICA. FFR assessment is an invasive accurate diagnostic tool to determine the physiological significance of a coronary lesion and distinguishes ischemia-producing lesions from those that do not; a significant reduction in FFR was defined as less than 0.80. The conclusion of the study was that an MPRI (cf. Section 5.2.2) value of 1.9 was the best threshold for the prediction of an FFR of 0.80. From these 50 patients, only 35 also underwent CTCA before PMR, with an interval of 41 ± 37 days between CTCA and PMR examinations. All the images were acquired at Erasmus MC, University Medical Center Rotterdam (Rotterdam, the Netherlands) between October 2007 and April 2008.

For evaluation of the SMARTVis tool, we included patients who match the following inclusion criteria. First, there should be a correlation between the true-positive and true-negative MPRI and FFR measurement. Also, there should be suspected stenoses in at least 2 of the 3 main coronary arteries using ICA, and a minimum of 1 significant stenosis and a maximum of 2 significant stenoses using FFR. Following these criteria, six patients that had false-positive or false-negative correlation between MPRI and FFR measurement, five who had no significant stenosis (i.e. the FFR was > 0.8 for the suspected lesions), 19 who had suspected stenoses in only one vessel using ICA and one that had triple-vessel disease using FFR were excluded. Finally, this resulted in a selection of 4 patients for the evaluation of our integrated visualization tool (Table 5.1).

CTCA images were acquired with a dual-source CT scanner (Somatom Definition, Siemens Medical Solutions, Forchheim, Germany). A tube voltage of 120 kV was used. All datasets were acquired with ECG-pulsing. Diastolic reconstructions were used, with reconstruction intervals ranging from 250 to 400 ms before the R-peak. The data were reconstructed using a smooth (B26f) kernel. The mean voxel size of the datasets is $0.32 \times 0.32 \times 0.4 mm^3$.

PMR images were acquired using a 1.5 Tesla MRI scanner (Signa CV/i, GE Medical Systems, Milwaukee, Wisconsin), with a cardiac eight-element phased-array receiver coil placed over the thorax (Signa CV/i, GE Medical systems, Milwaukee, Wisconsin USA). Cine cardiac PMR imaging was performed with a steady-state free precession technique

Table 5.1: Patients selected for the evaluation of the SMARTVis tool. Hemodynamically significant stenosis are indicated in bold (FFR < 0.8).

Patient	Sex	Age	ICA suspected stenosis	FFR
patient02	M	78	LAD	0.82
			LCX	**0.57**
patient10	M	63	**LAD**	**0.73**
			LCX	1.0
patient25	M	53	**LAD**	**0.75**
			LCX	0.94
			RCA	**0.73**
patient37	M	74	**LAD**	**0.74**
			RCA	**0.74**

(FIESTA). A first bolus of contrast media (Gadolinium diethyltriaminepentaacetic acid, Magnevist, Schering, Germany) was injected and rest first pass perfusion images were acquired. The temporal resolution per slice of 120 ms allowed imaging of 3-5 slices per R-R interval. Fifteen minutes after rest perfusion imaging, vasodilatation was induced by adenosine and a second bolus of contrast media was injected; stress first pass perfusion images were acquired, using the same pulse sequence and the same orientations used for rest perfusion.

5.3.2 Case-study design

To investigate the benefits of the proposed comprehensive visualization tool for assessing CAD, we performed a case-study evaluation on the four selected patient datasets, according to the guidelines presented by Yin [270]. First, we describe the case-study setup, then the patient analysis is described (i.e. the observers' diagnosis) and discussed.

Our main study question was defined as: "How can the comprehensive visualizations proposed in the SMARTVis tool assist radiologists/cardiologists in analyzing multimodal imaging data in the assessment of coronary artery disease?", and the case was defined as: "Use of the SMARTVis tool by two domain scientists referred to as RJvG, an expert cardiologist in MR imaging with over 10 years experience, and AR, a fellow student in radiology, expert in CTCA imaging with 3 years experience". The different functionalities of the SMARTVis tool were explained by the first author to the experts in a training session, using images of one of the excluded patient datasets; the tool was operated by the clinical expert during the evaluation. Both RJvG and AR are co-authors of this paper; they contributed to this work by providing feedback on our prototypes and clinical inputs, but did not work on the implementation itself. Thus, their role as case-study subjects was not compromised.

Our evaluation was divided into two parts: 1) conventional analysis, and 2) analysis using the SMARTVis tool. The comparative diagnostic study was performed on two different days, with a one-day interval, to limit the influence of the previous session. The patient's data were also analyzed in a different order: patient02, patient10, patient25, patient37 during the conventional analysis, and patient10, patient02, patient37, patient25 during the analysis using the SMARTVis tool. Beforehand, a number of case-study

Table 5.2: Comparative diagnostic study made using the conventional tools or the SMARTVis tool. List of the vessels which were referred for ICA. Only vessels with an FFR < 0.8 are listed.

Patient	Conventional tools		SMARTVis tool		FFR
	RJvG	AR	RJvG	AR	
patient02	-	LAD	LAD	LAD	-
	LCX	LCX	LCX	LCX	LCX
	RCA	-	-	-	-
patient10	LAD	LAD	LAD	LAD	LAD
	-	-	-	-	-
	RCA	-	-	-	-
patient25	-	-	LAD	LAD	LAD
	LCX	-	-	-	-
	RCA	RCA	RCA	RCA	RCA
patient37	LAD	LAD	LAD	LAD	LAD
	LCX	-	-	-	-
	RCA	RCA	RCA	RCA	RCA

propositions were defined to answer the main study question. During the evaluation sessions, we collected feedback on the usability of the tool, according to the study propositions. In Section 5.3.3, each proposition is stated, together with the expert's feedback, and discussed.

On the first day, together with each expert, in two separate sessions, we analyzed the four selected patient's multimodal imaging data using conventional tools. For each patient, the CTCA image was first inspected using an axial view and the MPR views of the annotated vessels. The expert was asked to list the positions and degree (< 50%, 50% − 70% or > 70%) of all visually significant stenoses detected on CTCA. Then, the rest/stress perfusion sequences were visually analyzed and the expert's decision was also supported by the TICs and perfusion BEP. Here, the expert was asked to list all the suspected ischemic regions. Finally, by mentally combining information from CTCA and PMR data, the expert assigned each of the listed suspected ischemic regions to a specific coronary artery lesion and made a decision concerning which coronary artery(ies) should undergo ICA and possible revascularization. On the consecutive day, the experts analyzed the patient's multimodal imaging data using our SMARTVis tool. Using the automatic stenosis detection and quantification, as well as the color-coded vessel model, in addition to the MPR view of the vessels, the significant stenoses were again listed by the expert. The suspected ischemic regions detected previously were reported and, using our 2D and 3D comprehensive model as well as the coronary perfusion territories, the expert again assigned each of the listed suspected ischemic region to a specific coronary artery lesion and made a new decision concerning which coronary artery(ies) should undergo ICA and possible revascularization.

The 2D and 3D comprehensive visualization models are shown in Figures 5.8-5.11 and the results of the comparative diagnostic study are presented in Table 5.2.

During the analysis of patient02, RJvG assigned an apical inferoseptal and inferior perfusion defect to a stenosis in the RCA using the conventional tool. However, with ICA and FFR, no significant stenosis was detected in the RCA; using the SMARTVis

tool, the same perfusion defect was assigned to a stenosis in the LAD (Figure 5.8). An obstruction in the LAD was indeed suspected using ICA, but the FFR indicated that it was not hemodynamically significant (FFR = 0.8). However, as RJvG considered the stenosis in LAD significant based on CTCA data; he thus decided to assign this apical inferoseptal and inferior perfusion defect to this LAD lesion. It should be noted that the lesion in LAD was calcified and the one in the LCX was not. The stenosis degree of calcified lesions in CTCA can be over-estimated due to imaging artifacts, while the non-calcified plaques are usually less easily detected and assessed. AR detected many more ischemic regions than RJvG for this patient, in the anterior and anterolateral wall; thus, AR referred ICA of the LAD, in both analyses. Nevertheless, it should be noted that the FFR value of the LAD (FFR = 0.82) is close to the cut-off value (FFR = 0.8) used to discriminate hemodynamically significant and non-significant lesions.

During the analysis of patient10, RJvG assigned an inferoseptal perfusion defect to a borderline stenosis in the RCA when using conventional tools, while, when using the coronary perfusion territories provided by the SMARTVis tool (Figure 5.9), the same perfusion defect was linked to the LAD; the LAD is indeed the coronary which is feeding the inferoseptal myocardium region of this patient and actually causing the perfusion defect ($FFR_{LAD} = 0.73$). The diagnosis of AR was correct in both analyses.

During the analysis of patient25, RJvG assigned a perfusion defect in apical inferior and inferoseptal wall to the RCA (resp. LAD) and in the inferolateral wall to the LCX (resp. RCA) using the conventional (resp. SMARTVis) tool; this patient has a right-dominant system, thus the RCA is feeding a larger area. In that case also, the coronary overlay and perfusion territory map helped him to correct his diagnosis. Similarly, AR misclassified the perfusion defect in the inferoseptal wall to the RCA, missing the significant stenosis in the LAD with the conventional tool, but reaching a correct diagnosis using the SMARTVis tool.

During the analysis of patient37, RJvG assigned a perfusion defect in the apical slice to the RCA instead of the LAD and a mid-anterior defect to the LCX instead of the LAD, using the conventional tool. These errors were corrected with the SMARTVis tool. AR made the same diagnosis using both tools.

In general, RJvG changed his diagnosis in all four cases and AR in one; the diagnosis of RJvG improved in three of the four cases and AR in one. Table 5.2 shows that there is no variability between the diagnosis of both observers with the SMARTVis tool, whereas, during the conventional evaluation, the observers had disagreement on one or two vessel(s) per patient. All the diagnoses were correct after using the SMARTVis tool, except for one case. The diagnosis of *patient02* remained incorrect, owing to overestimation of the degree of stenosis or overestimation of the number of abnormal perfusion regions during the analysis by the observers.

To conclude, when using the SMARTVis tool, a more reliable estimation of the correlation between perfusion deficits and stenoses led to a more accurate diagnosis, as well as a better inter-observer diagnosis agreement, which demonstrates the reproducibility of the results obtained with the SMARTVis tool. Thus, systems that integrate coronary anatomy and myocardial perfusion information may provide new opportunities for the risk assessment, diagnosis and management of patients with CAD.
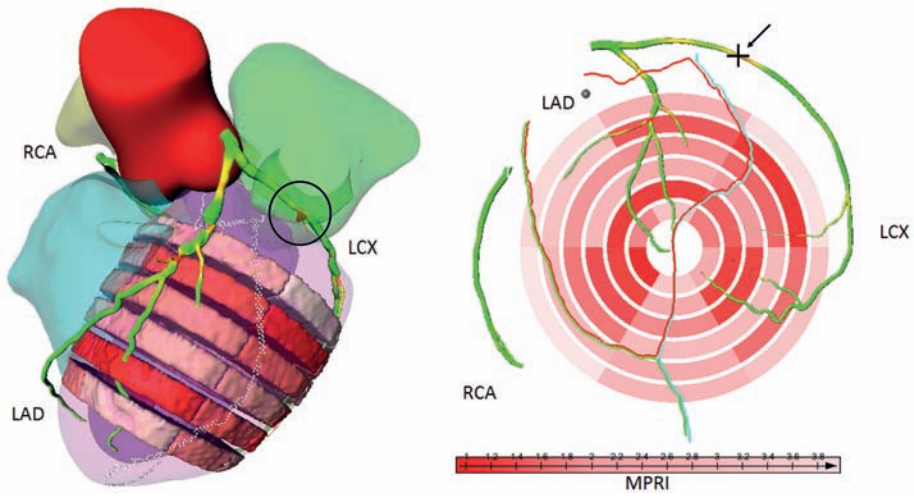
Figure 5.8: Patient02 - On ICA, suspected stenoses (30%) were visually detected in both LAD and LCX. Based on the FFR measurement, only the stenosis in the LCX was significant ($FFR_{LCX} = 0.57$) while the stenosis in the LAD was not considered to be significant ($FFR_{LAD} = 0.82$).
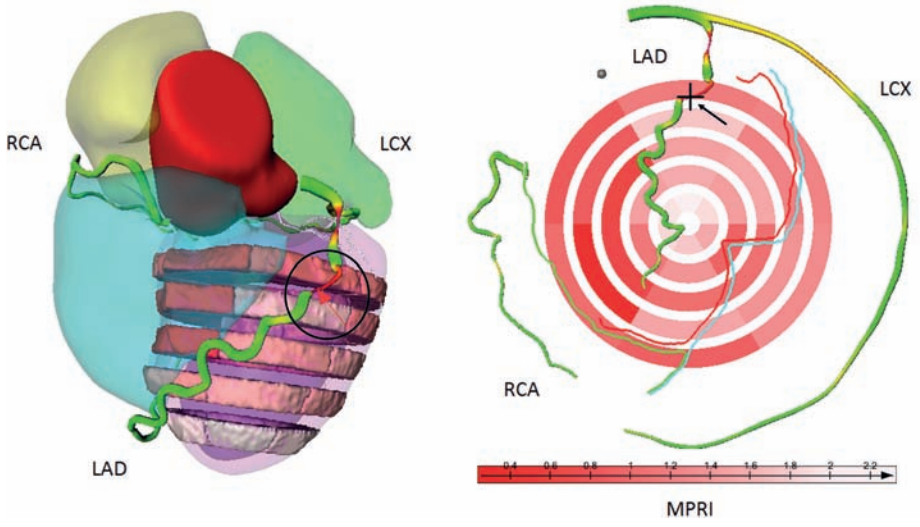
Figure 5.9: Patient10 - On ICA, suspected stenoses (30%) were visually detected in both LAD and LCX. Based on the FFR measurement, only the stenosis in the LAD was significant ($FFR_{LAD} = 0.73$) while the stenosis in the LCX was not considered to be significant ($FFR_{LCX} = 1.0$).
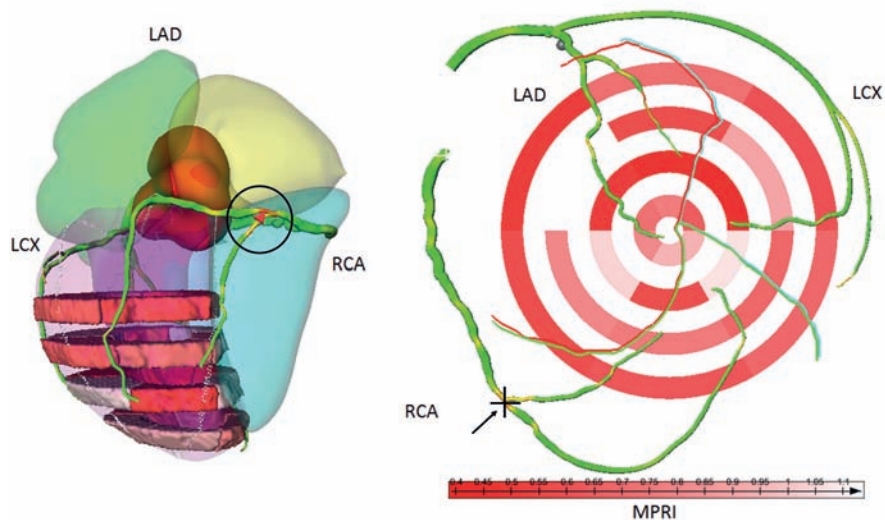
Figure 5.10: Patient25 - On ICA, suspected stenoses (30%) were visually detected in the three main arteries (LAD, LCX and RCA). Based on the FFR measurement, only the stenoses in the LAD and RCA were significant ($FFR_{LAD} = 0.75$, $FFR_{RCA} = 0.73$) while the stenosis in the LCX was not considered to be significant ($FFR_{LCX} = 0.94$).
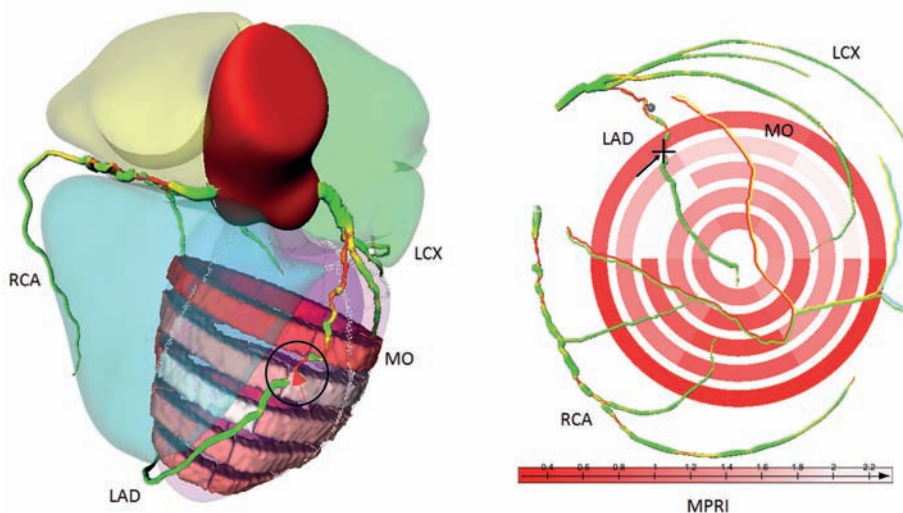
Figure 5.11: Patient37 - On ICA, suspected stenoses (30%) were visually detected in LAD and RCA. Based on the FFR measurement, both stenoses were indeed significant ($FFR_{LAD} = 0.74$, $FFR_{RCA} = 0.74$).

5.3.3 Expert feedback

The comparative diagnostic study demonstrated the clinical added value of the SMARTVis tool. Nevertheless, the experts' feedback is useful to understand *why* and *how* the SMARTVis tool performs better than the side-by-side analysis; this feedback complements the experiments. It should be noted that the experts' feedback is influenced by their personal preferences, based on years of experience and domain of expertise, which provide little basis for generalization.

Below, each case-study proposition is stated, together with the experts feedback, and then discussed.

The projection of the coronary artery tree on top of the 2D BEP facilitates the correlation between stenosis and ischemic myocardial region.

Both RJvG and AR agreed. RJvG emphasized that the anatomy varies greatly between individual and, thus, no standard correlation can be used. It also helped AR to better understand which myocardial territory belongs to an obstructive coronary stenosis.

The integrated visualization of the perfusion information in the 3D model of the heart facilitates the correlation between stenosis and ischemic myocardial region.

RJvG considered this to be an important part of the tool. Having an anatomical context (particularly for the right ventricle) to understand the location of the perfusion sectors and the position of the arteries with respect to the cardiac anatomy was appreciated. Such an anatomical context is not available in the 2D representation. RJvG did make the suggestion to extend the tool with the option to hide selective perfusion BEP sectors in order to look more closely at a region of interest. Although AR agreed, she did not use the 3D model during her analysis.

The color-coding of the degree of vessel stenosis facilitates the localization of interesting areas in terms of coronary disease, and the automatic stenosis ranking helps to further refine the location and quantification.

Although both of them agreed, RJvG explained that, with regard to the current resolution of CTCA technology, he would interpret the results derived from automatic vessel segmentation with caution. With improvement in CTCA resolution, he might have more confidence in the automatic stenosis grading. Similarly, AR used it mainly as verification: first, she analyzed and detected/quantified stenoses using the MPR vessel view; then, she compared her position/ quantification with the estimations provided by the tool. However, they both agreed that the color coding is useful to obtain a first impression about the extent of the disease.

Automatic position synchronization between MPR vessel viewer and the 2D and 3D models facilitates analysis of the data.

Both RJvG and AR agreed; for instance, when they wanted to refine their analysis to relate a perfusion defect with a particular artery, they visualized the suspected vessel on the MPR viewer while moving the cursor to see the corresponding location with respect to the cardiac anatomy and perfusion sectors.

The 3D model of the heart primarily helps in the interpretation of the coronary tree projection on the 2D model.

RJvG agreed, the 2D projection of the coronary tree seems to him to be too much distorted and the interpretation is difficult; he had a problem in to recognizing the different arteries. Thus, the 3D model, synchronized with the 2D model and the MPR view, supported his interpretation. AR also agreed, but did not really need the 3D model to interpret the 2D

representation. After one patient analysis, she stated that she was used to this model and was able to perform visual analysis using the 2D model only.

The coronary perfusion territory map and boundaries help in a patient-specific way to relate an ischemic segment to a particular vessel stenosis.

RJvG confirmed that, in general, it is very difficult to make a decision concerning which coronary artery is actually supplying the septal wall. Moreover, due to contrast limitations, the septal arteries are difficult to segment. Thus, experts usually have to rely on models, which generate considerable error, as in the case of patient 10 and 25 where septal perfusion defects were assigned to the RCA instead of the LAD. Therefore, this functionality was important to him. AR agreed with the proposition; however, the 2D projection of the arteries onto the 2D BEP already gave her an indication about perfusion territories.

The 2D representation is your preferred view for investigating relations between stenoses and ischemic myocardial regions.

RJvG disagreed; the 2D model is too distorted, making his interpretation really difficult. In contrast, AR agreed; currently, she is used to work with 2D maps of the LV. Especially for relating a certain perfusion defect to a particular artery, AR used mainly the 2D viewer.

The 3D representation is your preferred view for investigating relations between stenoses and ischemic myocardial regions.

RJvG agreed; he likes having anatomical information, such as the heart model. During the analysis, RJvG first navigated within the 3D model of the heart (with the color coded vessel model), to get an idea of the patient-specific anatomy and the position of the coronaries with respect to the left and right ventricles. Then, he incorporated the perfusion information into the 3D model and related perfusion defects with obstructive disease. AR used the 3D viewer only to see the position of suspicious stenoses detected on MPR images; she did not use it to relate anatomical and functional data.

To conclude, concerning the most informative visualization, RJvG preferred the integrated 3D model whereas AR chose the 2D projection model. Regarding the coronary perfusion territories, although both observers could mentally determine which region is supplied by which artery, they both found the automatic boundary delineation very useful in making a decision for borderline cases. The color-coding of the degree of stenosis was primarily appreciated to obtain a quick overview of the patient's disease state. Finally, the automatic stenosis detection/quantification strengthened the observer CTCA analysis.

5.4 Discussion, limitations and future work

We have proposed and evaluated a tool for comprehensive visualization of cardiac multimodal data. The results of a case-study with two experts in four patients demonstrated that integration of multimodal data in a common reference space supports the expert's diagnosis, by providing a more reliable estimation of the relation between perfusion deficits and stenoses, which led to a more accurate diagnosis as well as to a better inter-observer diagnosis agreement. However, some aspects can be improved.

In the fusion step of our processing pipeline, we used a registration approach (i.e. ICP) to spatially align CTCA with PMR data. The alignment of the data for each patient was visually verified, but small registration errors could still be present. One source of error arises from the left ventricle segmentation errors in CTCA and PMR. Another source of registration error originates from integrating different cardiac phases as obtained by CTCA and PMR images: PMR images are generally acquired during systole, whereas CTCA images are typically acquired at mid-diastole. During the fusion process, we did not

compensate for the fact that the images were acquired during different time points in the cardiac cycle. The accuracy of the registration, and the impact of registration errors on the diagnosis, remains to be investigated.

The visualization of coronary perfusion information, as proposed in this work, supported the expert diagnosis during the evaluation. Regarding the experts' feedback, it was shown that the coronary artery tree projection on top of the 2D perfusion BEP, or the integration of the perfusion into the 3D model, already significantly supported the expert while making the diagnosis. However, there is room to improve the estimation of the perfusion territories, as our estimation is now solely based on distances to segmented coronary arteries. Studies on blood flow simulation in coronary arteries have shown that the radius of the vessel also influences the amount of blood flowing through the artery. Computing the perfusion coronary territories using a *validated* perfusion simulation model would therefore be preferred.

In the CT imaging technique, calcifications in the vessel wall can appear significantly larger than they actually are, due to their high density and the relatively limited intrinsic resolution of the CT acquisition. This is known as the blooming effect and it hampers the assessment of stenoses, especially in small arteries. Because calcifications appear larger than they actually are, this artifact can result in an over-estimation of the degree of stenosis. The effect of this, and other CT imaging artifacts on our automatic stenosis detection and quantification method remains to be investigated.

Nevertheless, our preliminary clinical validation study demonstrates that the errors induced by the different processing step of our pipeline affect the final diagnosis accuracy to a lesser extent than the error in assuming a standard physiological model. During the side-by-side analysis of CTA and PMR data, the diagnosis derived by assuming a standard physiological model leads to errors in the assignment of a perfusion defect to a culprit artery; these errors can be prevented when using the SMARTVis tool.

Our study also demonstrates that the SMARTVis tool offers an added diagnostic value when assessing CAD in intermediate risk patients (i.e. with suspected stenoses in at least two of the main arteries). As stated in the Introduction, such a tool is not expected to improve the diagnosis in low-risk patients (i.e. single-vessel disease patients) as only one culprit artery can be assigned to the perfusion defect; moreover, it is unlikely to be used for triple-vessel disease patients (i.e. very-high-risk patients), as they are generally directly referred for revascularization. However, the SMARTVis tool is suitable for visual analysis of patients with all disease state. The same visualization technique can be used to interpret anatomical and functional information of single and triple-vessel disease patients in an integrated display. To what extent this would facilitate the diagnosis for these cases remains to be investigated; nevertheless, visualizations derived from the SMARTVis tool can be included in the patient report, to provide a quick overview of the patient's disease state.

Concerning our case-study evaluation, although the expert feedback was positive and the results were consistent, we need to conduct a larger study, also involving multicenter expert clinicians, in order to draw stronger conclusions. This will be considered for future work.

The time required to diagnose a patient has not yet been recorded; thus, we cannot state whether the SMARTVis tool allows a more efficient process of diagnosis. However, investigating whether making a diagnosis using the SMARTVis tool would be faster than it is nowadays using conventional tools should be part of a larger evaluation study.

After the evaluation, both experts were enthusiastic about the presented integrated visualization tool and were eager to use the SMARTVis tool in clinical practice. In our implementation, we use a generic data representation, and were able to import data from various research-oriented packages. Deployment of our tool for daily clinical use would therefore require only a further automation of the various processing steps. Additionally, the output of other software used in clinical practice can easily be integrated in the SMARTVis framework, provided that a conversion to our data representation can be performed. At present, most of the steps are performed using individual research oriented software packages. Nevertheless, a generic data representation was used when implementing the user interface. Therefore, the anatomical and functional information can be computed using any software used in daily clinical practice; a conversion to our representation would allow the information to be imported in the SMARTVis framework.

5.5 Conclusions

We have presented a complete pipeline for comprehensive analysis and visualization of multimodal cardiac imaging data (i.e. CTCA and PMR data).

The SMARTVis tool allows to efficiently establish a spatial correspondence between obstructive coronary artery lesions and myocardial regions with perfusion defect, in a patient-specific way. The location of coronary stenoses and perfusion abnormalities can be visualized jointly in 2D and 3D, thereby facilitating study of the relationship between the anatomic causes of an occluded artery and the physiological effects on the myocardial perfusion.

In addition, we investigated the benefits of the comprehensive visualizations in assessing CAD through a comparative diagnostic study and a case-study research evaluation, conducted together with two clinical experts. It has been confirmed that such comprehensive visualizations allow to effectively relate perfusion defects and coronary lesions. Moreover, it has been demonstrated that the analysis leads to a more accurate diagnosis.

For future work, we plan to extend our tool in two directions. First, we would like to integrate more functional information, such as scar tissue extracted from late enhancement MRI data, wall motion abnormalities detected on short-axis MRI data, and calcium scoring extracted from CT data. Then, the generic setup of the SMARTVis concept enables extension to other perfusion modalities, such as SPECT and CT perfusion imaging. Altogether, this would enable a 'one-stop-shop' visual exploration of functional, anatomical and perfusion data of the heart, which would maximally exploit the complementarities of all available data.